Cancer Research and Medicine
DOI: https://doi.org/10.63626/y0xgz932
ISSN Online: 3104-4131
ISSN Print: 3135-2715

Research Article

Preclinical investigations validate anticancer effects of alkyl-phospholipid perifosine against breast cancer cells

Marriyam Nasim[1], Iram Amin[1], Iqra Nasim[2]
1. Center of Excellence in Molecular Biology, University of the Punjab, Lahore, Pakistan
2. Environmental Sciences Department, University of Lahore, Lahore, Pakistan

Abstract
Background: Breast cancer is the most diagnosed cancer among women worldwide and a leading cause of cancer-related mortality. It arises from the uncontrolled growth of cells in the breast tissue, most often in the ducts or lobules. Major risk factors include genetic predisposition, hormonal influences, increasing age, and lifestyle factors. Early detection through screening methods such as mammography significantly improves treatment outcomes and survival rates. Despite advances in diagnosis and therapy, breast cancer remains a major public health challenge globally.
Methods: Breast cancer cells MCF-7 were cultured and treated with perifosine for further experiments. Cell viability was evaluated using the MTT assay. Nuclear morphology and apoptosis were assessed by DAPI staining. Cell migration was examined using scratch wound-healing assay. Gene expression analysis of selected genes was performed using real-time PCR. Data sets were compared between treated and untreated control groups.
Results: Perifosine treatment significantly reduced cancer cell viability in a dose-dependent manner as determined by the MTT assay. DAPI staining revealed prominent apoptotic features including nuclear condensation and fragmentation in treated cells compared to untreated controls. The scratch assay demonstrated a marked inhibition of cell migration, indicating reduced metastatic potential following perifosine exposure. Furthermore, real-time PCR analysis showed altered expressions of apoptosis (Caspases, *BAX*, *BCL2*), proliferation (cyclins and cell cycle inhibiters), stress (*GADD* genes) and transcription factors (*E2F*) supportive pro-apoptotic and anti-proliferative effects of perifosine.
Conclusion: The findings suggest that perifosine exhibits significant anticancer activity *in vitro* and require further investigations to explore clinical relevance.
Key Words: Breast cancer, Alkyl-phospholipids, Perifosine, Anticancer, Apoptosis, Cell cycle

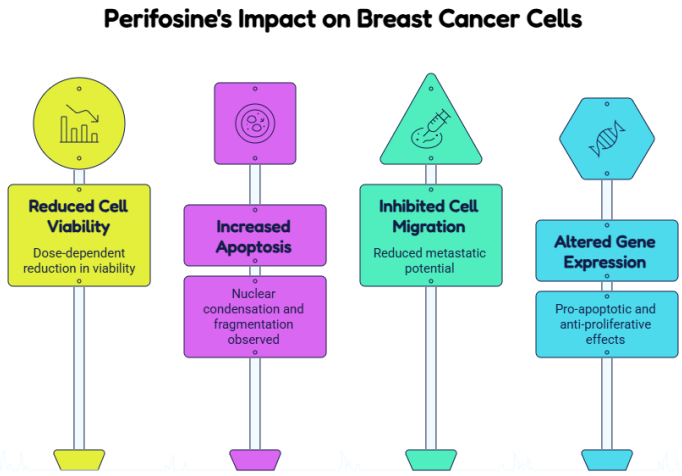

Corresponding Author: Marriyam Nasim
Email: marriyam.nasim@cemb.edu.pk
Received: 15.03.2026
Revised: 30.08.2026
Accepted: 31.08.2026
Published: 07.09.2026

INTRODUCTION

Breast cancer is a common cancer among women worldwide. It is a major cause of cancer associated mortality [1]. When abnormal breast cells grow without cell cycle control, the cancerous mass develops and may spread to distant parts of the body [2]. Early detection and diagnosis are very important for the required survival and treatment outcomes [3]. Treatment of breast cancer depends on molecular type and stage of breast cancer [4]. Treatment may include surgical removal of the diseased tissue, use of chemotherapy, radiotherapy along with specific options like hormonal, targeted or immunotherapy [5, 6]. Advances in targeted and personalized treatments have come up with improved outcomes. However, the strategies still cause psychological and physical side effects [7]. Furthermore, recurrence and resistance towards adopted therapy is also witnessed [8]. Currently, major challenges include limited access to healthcare, inadequate medical facilities, high treatment costs and limited outcomes [9]. Improving early detection, patient education and access to effective treatment are essential for reducing breast cancer mortality. Thus, along with developing new medicinal entities, repositioning existing molecules is effective domain to be explored [10].

Alkyl-phospholipids (APLs) are synthetic lipid analogues and have attracted considerable attention of the scientific community as potential anticancer molecules [11]. Unlike conventional chemotherapeutic agents, APLs interfere with the cell membrane content and lipid metabolism [12]. This leads to inhibition of the tumor cell proliferation followed by antitumor effects [13]. On cell level, APLs alter signaling pathways required for cell proliferation, survival and cell membrane mediated enzyme activity [14]. These effects of APLs are tumor cell specific and show selectivity toward rapidly proliferating cancer cells [15]. APLs have demonstrated anticancer effects against different tumor types including breast, leukemia, prostate and colorectal in preclinical *in vitro* and *in vivo* investigations [16-19]. However, therapeutic applications of the different classes of the APLs have demonstrated limited and variable efficacy and toxicity [20]. To explore this class of molecules as anticancer medicines, further research is required to clarify the specific impact of different members of this group.

Perifosine is the second-generation molecule of APLs, oral antitumor agent and has been investigated for potential anticancer activity [21]. Perifosine affects cell signaling primarily by inhibiting Akt (protein kinase B) which is an important member of the PI3K/Akt pathway [22]. PI3K/Akt pathway regulates key functions including cell proliferation, metabolism, survival and apoptosis [23]. By targeting Akt signaling, perifosine suppress the tumor cell growth and induce apoptosis [24]. It is further noted that this molecule can enhance the sensitivity of cancer cells towards other anticancer agents, when used in combination [25]. *In vitro* studies have shown its activity against different types of cancer like multiple myeloma, leukemia and solid tumors [26-28]. Although clinical studies have demonstrated variable efficacy of perifosine, it is still an important therapeutic candidate particularly for tumorous where PI3K/Akt signaling is dysregulated.

Purpose of this study was to investigate anticancer effects of perifosine against breast cancer cells in the preclinical setting. Effects on breast cancer cell viability, proliferation, apoptosis and related genetic profiles were investigated. Overall objective was to determine potential of perifosine as a therapeutic agent against breast cancer and provide evidence supporting further investigation as targeted anticancer treatment.

METHODS

Cell Cultures

Human breast cancer cell line (MCF-7) was cultured under standard *in vitro* required culture conditions. The cells were maintained in appropriate complete growth medium (RPMI-1640) supplemented with fetal bovine serum (10% by volume) and antibiotics (streptomycin and penicillin). The cells were incubated at 37°C in humidified atmosphere supplied with 5% CO_2. The cultures were regularly monitored for cell growth and were sub-cultured when reached 70-80% confluency. For experimental needs, the cells in logarithmic growth phase were obtained and seeded as per required density.

Cytotoxicity Assay

Cell viability was monitored using MTT assay based on the ability of viable cells to reduce yellow MTT (3-(4,5-dimethylthiazol-2-yl)-2,5-diphenyltetrazolium bromide) into insoluble purple formazan crystals. Briefly, the breast cancer cells were seeded in 96-well plates at density of 5000 cells/100 µl/well and allowed to adhere before treatment with different concentrations of perifosine (1, 2, 4, 8, 16, 32 µM) for the selected incubation period (48 hours). MTT solution was then added to each well (10 µl/well) and incubated to allow formazan crystals formation. The resulting crystals were dissolved using an appropriate solubilizing solution (DMSO) and absorbance was measured at 570 nm using a microplate reader. Cell viability was expressed as a percentage of the untreated control. The experiment was performed in four replicates for each group.

Nuclear Staining

DAPI (4′,6-diamidino-2-phenylindole) staining was performed to evaluate nuclear morphological changes associated with apoptosis in breast cancer cells following perifosine treatment. Cells were seeded (50000 cells/1000 µl) in each well of 24 well culture plate. Cells were treated with desired concentrations of perifosine (10 µM) for specified incubation period (48 hours). After treatment, cells were washed with phosphate-buffered saline (PBS), fixed with an appropriate fixative (cold 70% ethanol), and stained with DAPI solution in the dark. DAPI binds to DNA and produces blue fluorescence, allowing visualization of nuclear morphology. The stained cells were examined using the fluorescence microscope (EVOS, Life Technologies) and apoptotic features such as chromatin condensation, nuclear fragmentation and formation of apoptotic bodies were assessed and compared with untreated control cells.

Migration Assay (Scratch Assay)

The wound-healing scratch assay was performed to evaluate the effect of perifosine on the migratory ability of breast cancer cells. Briefly, cells were seeded in 24 well culture plates (100000 cells/1000 µl/well) and grown to form a nearly confluent monolayer. A straight scratch was gently created across the cell monolayer using a sterile 200 µl pipette tip, followed by washing with PBS to remove detached cells. Fresh culture medium containing indicated concentrations of perifosine was then added (10 µM). Images of the scratched areas were captured at 0 hours and at selected time points (24 hours) using an inverted microscope (EVOS, Life Technologies).

The percentage of wound closure was determined by measuring the scratch area at each time point and comparing it with untreated control. Reduced wound closure in perifosine-treated cells was considered indicative of inhibited cell migration.

Expression Analysis (Real time PCR)

Primers for the selected target genes related to apoptosis (Caspases, *BAX*, *BCL2*), cell cycle (cyclins and cell cycle inhibiters), cell stress (*GADD* genes) and transcription factors (*E2F*) were designed using Primer3 software (Table 1). Primer specificity was confirmed using sequence database analysis. The primers were optimized by performing gradient PCR to determine the appropriate annealing temperature and amplification conditions, and PCR products were evaluated by agarose gel electrophoresis (data not shown here). For gene expression analysis, the cells were seeded (100000 cells/1000 µl) in each well of 12 well culture plates and were treated with desired concentrations of perifosine (10 µM) for the specified incubation period (48 hours). Afterwards, total RNA was extracted from control and perifosine-treated breast cancer cells and converted into complementary DNA using a reverse-transcription system (RevertAid First Strand, Thermo Scientific). Quantitative real-time PCR (qRT-PCR) was performed using gene-specific primers, master mix (SYBR Green, Thermo Scientific) along with a suitable housekeeping gene (HPRT1) used as internal reference. Relative gene expression was calculated using the comparative $2^{-\Delta\Delta Ct}$ method, and changes in expression between treated and control groups were analyzed.

Table 1. Primer sequences used for the amplification of target genes in this study.

Genes	Category	Forward Primer	Reverse Primer
BAX	**Apoptosis**	TCTGACGGCAACTTCAACTG	GGAGGAAGTCCAATGTCCAG
BCL2		GCCCTGTGGATGACTGAGTA	CGTACAGTTCCACAAAGGCA
CASP3		GAGGCCGACTTCTTGTATGC	AGCGTCAAAGGAAAAGGACT
CASP7		TTCCACGGTTCCAGGCTATT	AGTTCCTTGGTGAGCATGGA
CASP9		GAAAATGGTGCTGGCTTTGC	TCTTTCTGCTCCCCACCAC
E2F1	**Transcription and Stress**	GGGCTCTAACTGCACTTTCG	AGAAGTGCTCTCACCGTCCT
E2F6		TGCCTTCGCCATGAATCCTT	GGAGCCCATTCCTACATTCTCA
GADD34		GAGACTCCCCTAAAGGCCAG	GGGGCTAAAGGTGGGTTCC
GADD45A		AACGGTGATGGCATCTGAAT	CCCTTGGCATCAGTTTCTGT
GADD153		TCTTGACCCTGCTTCTCTGG	GCTGTGCCACTTTCCTTTCA
CCND1	**Cell Cycle**	GGGGGCGTAGCATCATAGTA	GTGGTGGCACGTAAGACACA
CCND2		GTCTCAAAGCTTGCCAGGAG	ATATCCCGCACGTCTGTAGG
CDKN1A		GCTTCATGCCAGCTACTTCC	CTGTGCTCACTTCAGGGTCA
CDKN1B		CCGGCTAACTCTGAGGACAC	TGCAGGTCGCTTCCTTATTC
CDKN2B		GACCGGGAATAACCTTCCAT	AAACCCTGAAAAGCAAACGA

RESULTS

Cytotoxic Effects of Perifosine

Cell viability, expressed as percentage of untreated control, showed almost a concentration-dependent response towards increasing treatment concentrations (1-32 μM) of perifosine. The untreated group (0 μM) viability was set to 100%, providing the reference level. At the lower concentrations (1-2 μM), viability increased slightly reaching approximately up to 110%. This modest increase suggests that low dose exposure produced a slight stimulatory response. A decline in viability became apparent as concentration increased beyond 2 μM. At 4 μM, viability decreased to approximately 87%, representing a reduction of about 13% relative to untreated control. A similar response was observed at 8-32 μM, where viability declined maximally to 66%, representing a reduction of about 34% relative to untreated control. Overall, the results demonstrate biphasic concentration-response pattern. Treatment at 1–2 μM was associated with slightly higher viability than the untreated control, whereas concentrations of 4-32 μM progressively reduced cell viability, with the strongest apparent effect occurring at 16 μM. The error bars indicate variability around the mean values, with relatively greater variability observed at 2, 4, 8, and 32 μM (Figure 1).

Apoptotic Effects of Perifosine

DAPI staining revealed differences in nuclear appearance and cell density between the control and perifosine treated group. In control field, numerous DAPI-positive nuclei were distributed throughout the image, with relatively high cellular density and predominantly rounded to oval nuclear profiles. Nuclei generally appeared comparatively uniform, consistent with preservation of nuclear morphology in untreated cells. In contrast, cells exposed to perifosine displayed an evident reduction in the number/density of DAPI-positive nuclei within the representative microscopic field. The treated cells were more sparsely distributed, with larger cell-free areas separating individual cells and clusters. In addition to this reduction in apparent cell density, the treated field showed greater heterogeneity in nuclear morphology. Several nuclei appeared more intensely condensed and were present in compact clusters, features that can be consistent with chromatin condensation and nuclear alterations associated with apoptotic cell death. Qualitatively, the control field therefore exhibited a dense and relatively uniform nuclear distribution, whereas perifosine treatment resulted in more heterogeneous nuclear patterns. These observations are consistent with the preceding viability and apoptosis-related findings, suggesting that exposure to perifosine adversely affected cell survival and altered nuclear morphology. However, an exact percentage reduction in cell number or increase in apoptotic nuclei cannot be calculated reliably from the presented images alone. Overall, staining provides qualitative morphological evidence that perifosine reduces apparent cell density and is associated with nuclear changes compatible with apoptosis compared with untreated control cells (Figure 2).

Antimigratory Effects of Perifosine

The wound-healing/scratch assay demonstrated a clear reduction in cell migration following treatment with perifosine compared with the untreated control over the 24 hours period. At 0 hours, both groups displayed a well-defined cell-free scratch region of broadly comparable appearance, providing baseline for assessment of subsequent wound closure. After 24 hours, control cells showed substantial migration into the scratched area, resulting in visible narrowing of the wound. In contrast, the perifosine-treated cultures retained considerably wider cell-free region, indicating impaired migration and reduced wound closure. Quantitative analysis supported microscopic observations. At 24 hours, the relative covered area was approximately 45% in control group, compared with only ~25% in cells treated with perifosine. Thus, the treatment produced an absolute reduction of approximately additional 20 percentage in the covered area. Relative to the control, this corresponds to an approximately 45% reduction in the wound coverage/migratory response. The error bars indicate variability between measurements, but the separation between the two groups remained pronounced. Importantly, the bracket and single asterisk (*) above the two groups indicate that the difference between control and perifosine-treated cells was statistically significant. The quantitative difference is consistent with the representative microscopy images, in which control cells migrated substantially farther into the initially cell-free region than perifosine-treated cells during the 24 hours period. Overall, these findings demonstrate that perifosine significantly inhibited wound closure over 24 hours, with the covered area decreasing from approximately 45% in controls to 25% following treatment. Collectively, the results are consistent with a marked inhibitory effect of perifosine on cellular migratory capacity under the conditions of the assay (Figure 3).

Expression Changes Induced by Perifosine

To figure out effects of perifosine exposure on expressional levels of genes, transcriptomic data was measured via real time PCR method. Treatment with perifosine produced marked alterations in the genes associated with apoptosis, cellular stress responses, and cell-cycle regulation compared with the control. Control values were set to 1 as base level 1.0%,

whereas perifosine exposure produced substantial target-dependent up- or down-regulation in the genes. For apoptosis-associated genes, perifosine increased the relative expression of *CASP3*, *CASP7*, *CASP9*, and *BAX* while markedly decreasing *BCL2*. *CASP3* increased modestly to 1.4fold, whereas *CASP7* exhibited a more prominent increase reaching 2.6fold. *CASP9* increased to approximately 2.0%, while the pro-apoptotic *BAX* gene increased to 2.1fold. In contrast, *BCL2* showed a pronounced decrease to approximately 3fold. Collectively, the simultaneous elevation of caspases and *BAX* and reduction of *BCL2* demonstrates a clear shift in the measured genetic profile toward pro-apoptotic signaling following perifosine exposure. Perifosine also altered genes involved in cellular stress and growth regulation. *GADD34* showed a prominent increase of ~3fold, while *GADD153* increased to 2.5fold. Conversely, *GADD45A* decreased to approximately ~1fold.

E2F transcription factors also displayed negative responses, with *E2F1* and *E2F6* decreasing to approximately 1.1fold. Pronounced changes were observed among the cell-cycle regulatory genes. The cyclin *CCND1* and *CCND2* decreased to ~1.1 and ~3fold, respectively. In contrast, the cyclin-dependent kinase inhibitor *CDKN1A* exhibited positive response and induced by 3.5fold. *CDKN1B* showed a moderate increase to 1.5fold, while *CDKN2B* increased to approximately 1.8fold. Opposing changes in cyclins and cyclin-dependent kinase inhibitors are consistent with suppression of cell-cycle progression. Taken together, observed expression pattern is consistent with a coordinated response involving enhanced apoptotic signaling, activation of stress-associated pathways, and inhibition of cell-cycle progression following treatment with perifosine (Figure 4).

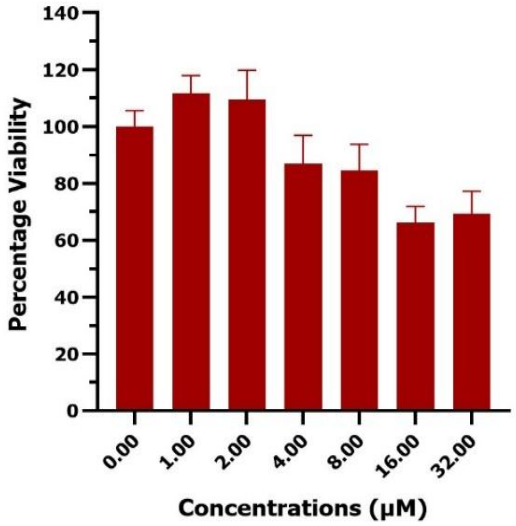

Figure 1. Effect of perifosine treatment on cell viability. Cell viability was assessed following exposure to increasing concentrations (1-32 µM) of the tested compound. Percentage viability showed a modest increase at lower concentrations (1-2 µM) followed by concentration-dependent decline at higher concentrations. Bars represent mean percentage cell viability, and error bars indicate variability among measurements.

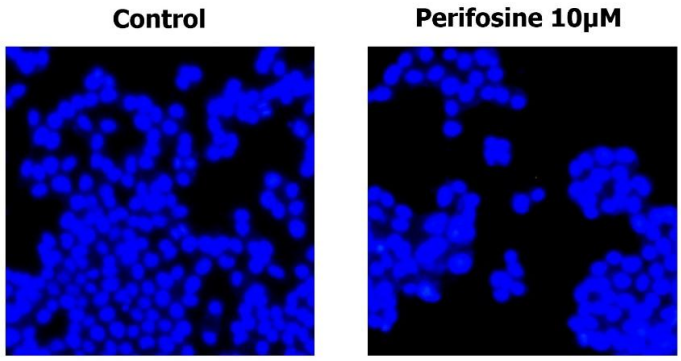

Figure 2. DAPI staining of control and perifosine treated cells. Representative fluorescence micrographs showing DAPI-stained nuclei (blue) in untreated control cells and cells treated with perifosine. Compared with the densely distributed nuclei observed in the control group, perifosine-treated cells exhibited an apparent reduction in cell density together with alterations in nuclear morphology, including nuclear condensation and clustering.

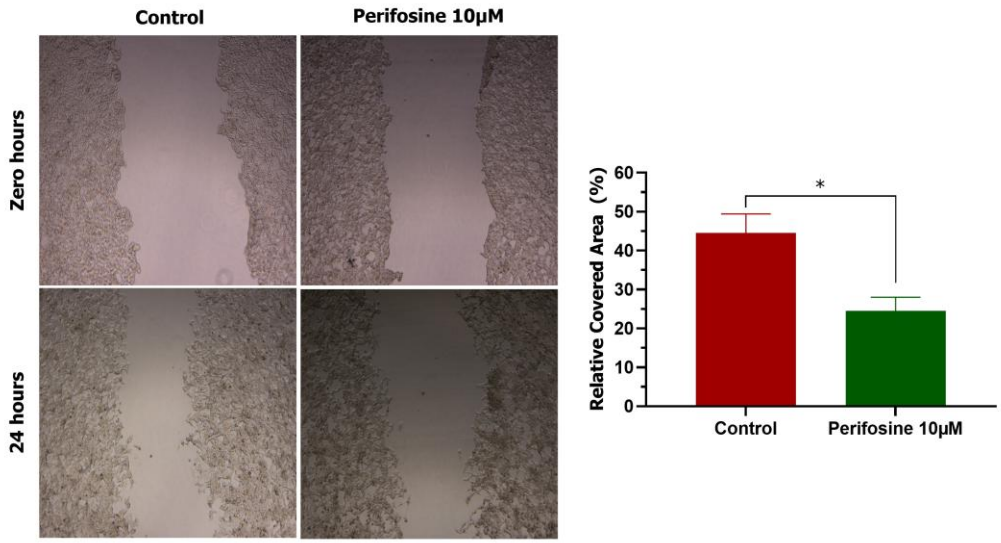

Figure 3. Perifosine inhibits cell migration in wound-healing assay. Representative phase-contrast images of untreated control cells and cells treated with perifosine at 0 and 24 h following scratch formation. At 24 hours, control cells showed greater migration into the scratched area, whereas perifosine-treated cells exhibited reduced wound closure. Quantification of the relatively covered area demonstrated significant reduction in cell migration following perifosine treatment compared with the control group ($P < 0.05$). Bars represent mean values with error bars indicating variability among measurements.

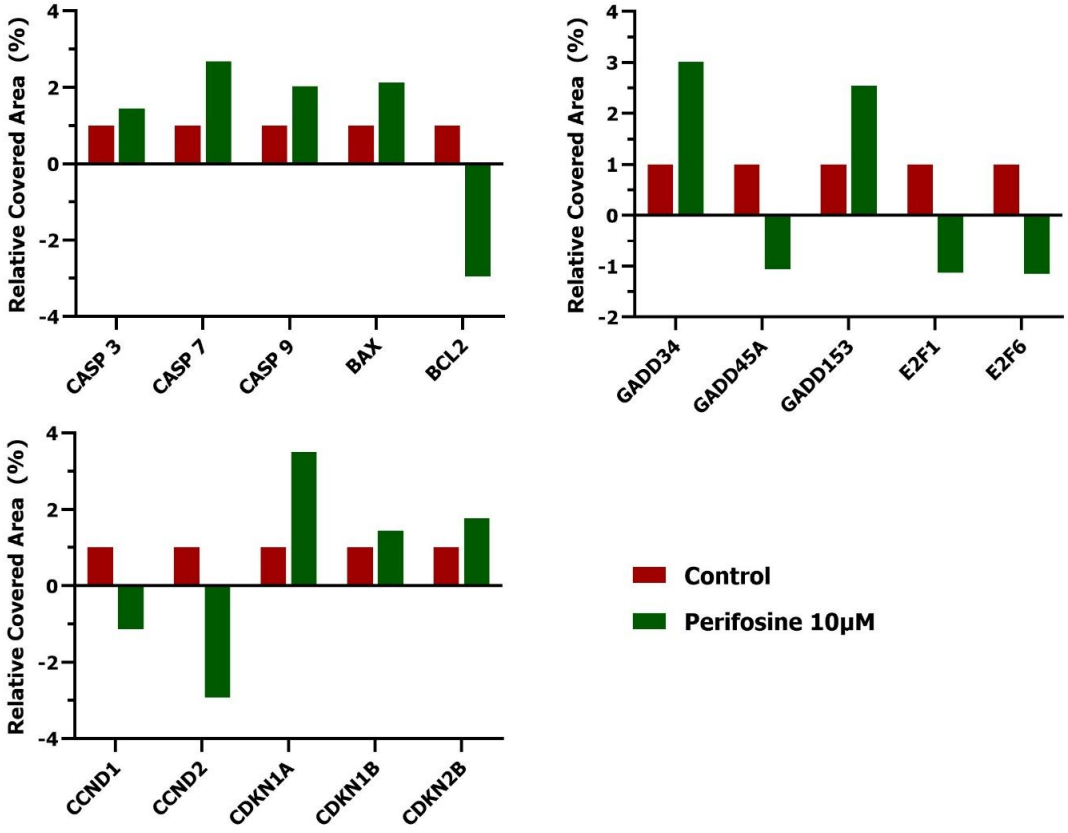

Figure 4. Effect of perifosine treatment on the relative expression of apoptosis, stress and cell cycle associated genes. Values are presented as relative fold changes as compared to untreated controls and were calculated by using Livak method. Perifosine increased the relative expression of pro-apoptotic and stress-associated markers, including *CASP3*, *CASP7*, *CASP9*, *BAX*, *GADD34*, and *GADD153*, while *BCL2*, *GADD45A*, *E2F1*, and *E2F6* showed reductions relative to the control. Among cell-cycle-associated markers, *CDKN1A*, *CDKN1B*, and *CDKN2B* increased, whereas *CCND1* and *CCND2* decreased following perifosine treatment.

DISCUSSION

Objective of study was to identify the antineoplastic effects of perifosine against the breast cancer cells at functional and molecular levels. The present findings indicate that perifosine produces concentration dependent reduction in cellular metabolic viability, although the response was not strictly monotonic across entire concentration range. Relative viability was set to 100% in untreated cells and declined maximally to 66% at 16 μM concentration. Thus, the principal biological effect becomes apparent above 2 μM, with the largest loss of viability occurring at 16-32 μM. Studies have demonstrated concentration and time-dependent inhibition of tumor-cell growth following perifosine exposure. For example, prostate cancer PC-3 cells showed progressively reduced viability with increasing perifosine concentrations between 1 and 20 μM, while hepatocellular carcinoma models similarly demonstrated time- and dose-dependent reductions in the proliferation following treatment with 5-40 μM perifosine [29, 30]. The decline observed here up to 66% at 16 μM therefore agrees with the general expectation that increasing perifosine exposure eventually compromises cancer-cell survival.

DAPI-staining results provided morphological evidence that exposure to perifosine alters nuclear organization and reduces the apparent density of cells compared with the untreated control. Control cultures contained numerous, relatively uniformly distributed DAPI-positive nuclei, whereas the perifosine-treated field contains fewer nuclei, larger cell-free regions, and more heterogeneous nuclear appearances. Some nuclei treated appeared more intensely condensed and clustered. Because chromatin condensation, nuclear shrinkage, and subsequent fragmentation are characteristic morphological features of apoptosis, these observations are consistent with an increase in apoptotic cell death following perifosine treatment. In hepatocellular carcinoma cells, treatment with perifosine produced similar characteristic DAPI-detectable apoptotic nuclear changes, including apoptotic-body formation, whereas untreated cells lacked evident apoptotic morphology. The same study demonstrated increased apoptosis by Annexin V/PI analysis together with activation of caspase-3 and caspase-9, supporting the interpretation that the nuclear alterations were associated with apoptotic cell death rather than being nonspecific morphological changes [30]. Nuclear alterations observed here could represent a downstream morphological consequence of disrupted pro-survival signaling. The apparent reduction in the number of DAPI-positive nuclei in the perifosine-treated field is also biologically relevant. This could reflect decreased proliferation, increased cell death and subsequent loss of cells during processing, or a combination of these mechanisms.

The scratch assay demonstrated that perifosine markedly suppresses wound closure over 24 hours. Although the control and treated cultures displayed broadly comparable cell-free gaps at 0 hours, a clear divergence was evident after 24 hours. Control cells migrated substantially into the scratched region, whereas a considerably wider gap persisted in the perifosine-treated cultures. Quantification data confirmed this observation, with covered area reaching approximately ~45% in the control but only ~25% following perifosine treatment. This corresponds to ~45% lower coverage relative to control. Importantly, the asterisk shown in the figure indicates that this reduction was statistically significant ($P < 0.05$). This inhibitory effect is broadly consistent with the established importance of PI3K/Akt pathway in cellular migration. Akt signaling contributes to cytoskeletal organization, cell survival, proliferation, and migratory behavior. Conversely, pharmacological interference with this pathway can suppress migration [31]. The present findings are particularly relevant because perifosine is a known Akt-pathway inhibitor. Published experiments have used perifosine specifically to interrogate Akt-dependent migratory responses [32]. Together, these observations are directionally consistent with the substantially reduced wound coverage observed in the present experiment. The magnitude of the effect is noteworthy as 10 μM of perifosine substantially compromises the processes contributing to closure of the artificial wound. From an oncological perspective, inhibition of these processes could be important because enhanced cellular motility is fundamental component of tumor invasion and metastatic dissemination. Thus, the current result suggests that the biological effects of perifosine may extend beyond suppression of cell viability to include inhibition of a phenotype associated with tumor-cell movement. However, reduction in the covered area cannot automatically be interpreted as a purely anti-migratory effect. A part of the reduced wound closure may arise from decreased proliferation or increased cell loss rather than impaired migration alone.

Functional changes at cell level are accompanied by expressional changes at genes levels. The present expression profile suggests that perifosine induced coordinated shift from proliferative/survival signaling toward cell cycle inhibition, cellular stress, and apoptosis. Three complementary patterns were evident: increased pro-apoptotic markers (*CASP3*, *CASP7*, *CASP9* and *BAX*) with decreased *BCL2*; induction of stress-associated *GADD34* and *GADD153* with suppression of *GADD45A*, *E2F1* and *E2F6*; and reduced *CCND1*/*CCND2* accompanied by increased *CDKN1A*, *CDKN1B* and *CDKN2B*. Taken together, these changes are biologically consistent with the

known antiproliferative actions of perifosine. Apoptosis panel provided one of the clearest indications of a shift toward a pro-death phenotype. Perifosine increased *CASP3* to ~1.5, *CASP7* to ~2.6 and *CASP9* to ~2, while *BAX* increased to ~2.1fold. Conversely, *BCL2* showed pronounced decrease to approximately 3fold. The opposing behavior of *BAX* and *BCL2* is particularly relevant because the balance between pro-apoptotic and anti-apoptotic *BCL2*-family signaling is important determinant of mitochondrial apoptotic susceptibility. The accompanying increases in initiator caspase-9 and executioner caspases-3/7 further support an apoptosis-associated response. In hepatocellular carcinoma cells, perifosine inhibited Akt phosphorylation and induced apoptosis accompanied by caspase-9 and caspase-3 activation, increased *BAX* and altered *BCL-2* associated signaling [33]. Similarly, medulloblastoma cells treated with perifosine showed cleavage of caspase-9, caspase-7 and caspase-3, providing a particularly close match to the caspase pattern observed in this study [34].

An equally striking pattern was evident in the cell-cycle panel genes. The proliferative cyclins *CCND1* and *CCND2* decreased to 1.1 and 3fold, respectively, whereas cyclin-dependent kinase inhibitors *CDKN1A*, *CDKN1B* and *CDKN2B* increased. *CDKN1A* showed the highest increase, reaching approximately 3.5fold followed by *CDKN2B* and *CDKN1B* with 1.8 and 1.5fold induction in response to perifosine exposure. This reciprocal pattern strongly suggests suppression of molecular machinery that normally supports cell-cycle progression. This particularly strong induction of *CDKN1A* is in agreement with the known effects of perifosine in literature. Perifosine has previously been shown to induce *CDKN1A* and produces cell-cycle arrest at the G1/S and G2/M boundaries. Importantly, experimental loss of *CDKN1A* prevented perifosine-mediated cell-cycle arrest in some models, indicating that *CDKN1A* can be a functional mediator rather than merely a secondary marker [35]. The reduction in *CCND1* is also mechanistically plausible in the context of Akt inhibition. Akt contributes to cell proliferation through several downstream regulators, including cyclin D1 and *CDKN1A*. Published hepatocellular carcinoma experiments have shown that perifosine-mediated inhibition of Akt is associated with altered cyclin expression, increased *CDKN1A* and cell-cycle arrest. Thus, the current combination of reduced cyclin D-family signals and increased CDK inhibitors is consistent with an antiproliferative state [36].

The *GADD/E2F* panel adds evidence that perifosine exposure produces a broader cellular stress response rather than affecting apoptosis alone. *GADD34* increased to approximately 3fold, while *GADD153* increased to approximately 2.5fold. *GADD153*, commonly referred to as CHOP, is strongly associated with cellular stress responses and can participate in pro-apoptotic signaling when stress becomes prolonged or unresolved [37]. Consequently, its elevation alongside increased caspases and reduced *BCL2* provides a link between cellular stress and subsequent apoptotic commitment. Conversely, *E2F1* and *E2F6* expressions decreased to 1.1fold, while *GADD45A* also declined to around ~1fold. The suppression of *E2F*-associated signals is compatible with the broader reduction in proliferative activity suggested by the cyclin/CDK-inhibitor profile. The decrease in *GADD45A* despite increases in *GADD34* and *GADD153* is important because it demonstrates that perifosine is not producing uniform activation of all stress-response genes. Rather, individual stress pathways appear to be differentially regulated. Such heterogeneity is biologically important given that perifosine has multiple cellular consequences and that its mechanism varies among tumor types.

CONCLUSION

Taken together, findings demonstrate that perifosine exerts coordinated antiproliferative, pro-apoptotic, and anti-migratory effects, supporting a multifaceted mechanism of action rather than an isolated effect on cell viability. The concentration-dependent decline in metabolic viability at higher perifosine concentrations was accompanied by DAPI-detectable nuclear alterations consistent with apoptotic morphology and a significant reduction in wound closure. At molecular level, increased *CASP3*, *CASP7*, *CASP9*, and *BAX* together with decreased *BCL2* indicate a shift toward pro-apoptotic signaling, while suppression of *CCND1* and *CCND2* and increased *CDKN1A*, *CDKN1B*, and *CDKN2B* are consistent with inhibition of cell-cycle progression. Concurrent alterations in *GADD* and *E2F* genes further suggest engagement of cellular stress and growth-regulatory pathways. Collectively, these observations are broadly consistent with previous literature describing perifosine as an inhibitor of Akt-associated survival signaling capable of promoting cell-cycle arrest and apoptosis in cancer cells. Convergence of viability, morphological, migratory, and molecular findings provide complementary evidence that perifosine disrupts several processes required for cancer-cell persistence and progression. Nevertheless, additional validations are required for confirming the proposed mechanisms and establishing the broader therapeutic significance of these findings.

REFERENCES

1. Gu H, Wang R, Beeraka NM, Lu P, Zhao X, Li L, Liu Y, Kandula DR, Fan R, Gayathri T, Nikolenko VN. Global burden and trends of breast cancer: GLOBOCAN 2022 estimates of incidence and mortality in 185 countries. Chinese medical journal. 2026 Feb 5;139(03):404-14.
2. Nolan E, Lindeman GJ, Visvader JE. Deciphering breast cancer: from biology to the clinic. Cell. 2023 Apr 13;186(8):1708-28.
3. Barrios CH. Global challenges in breast cancer detection and treatment. The Breast. 2022 Mar 1;62:S3-6.
4. Xiong X, Zheng LW, Ding Y, Chen YF, Cai YW, Wang LP, Huang L, Liu CC, Shao ZM, Yu KD. Breast cancer: pathogenesis and treatments. Signal transduction and targeted therapy. 2025 Feb 19;10(1):49.
5. Zhai J, Wu Y, Ma F, Kaklamani V, Xu B. Advances in medical treatment of breast cancer in 2022. Cancer Innovation. 2023 Feb;2(1):1-7.
6. Wang Y, Minden A. Current molecular combination therapies used for the treatment of breast cancer. International journal of molecular sciences. 2022 Sep 20;23(19):11046.
7. Tommasi C, Balsano R, Corianò M, Pellegrino B, Saba G, Bardanzellu F, Denaro N, Ramundo M, Toma I, Fusaro A, Martella S. Long-term effects of breast cancer therapy and care: calm after the storm?. Journal of clinical medicine. 2022 Dec 6;11(23):7239.
8. Khan MM, Yalamarty SS, Rajmalani BA, Filipczak N, Torchilin VP. Recent strategies to overcome breast cancer resistance. Critical Reviews in Oncology/Hematology. 2024 May 1;197:104351.
9. Trapani D, Ginsburg O, Fadelu T, Lin NU, Hassett M, Ilbawi AM, Anderson BO, Curigliano G. Global challenges and policy solutions in breast cancer control. Cancer treatment reviews. 2022 Mar 1;104:102339.
10. World Health Organization. Patient navigation for early detection, diagnosis and treatment of breast cancer: technical brief. World Health Organization; 2024 Oct 11.
11. de Almeida Pachioni J, Magalhães JG, Lima EJ, de Moura Bueno L, Barbosa JF, de Sá MM, Rangel-Yagui CO. Alkylphospholipids–a promising class of chemotherapeutic agents with a broad pharmacological spectrum. Journal of Pharmacy & Pharmaceutical Sciences. 2013 Dec 20;16(5):742-59.
12. Kaleağasıoğlu F, Zaharieva MM, Konstantinov SM, Berger MR. Alkylphospholipids are signal transduction modulators with potential for anticancer therapy. Anti-Cancer Agents in Medicinal Chemistry-Anti-Cancer Agents). 2019 Jan 1;19(1):66-91.
13. N Apostolova S, A Toshkova R, B Momchilova A, D Tzoneva R. Statins and alkylphospholipids as new anticancer agents targeting lipid metabolism. Anti-Cancer Agents in Medicinal Chemistry (Formerly Current Medicinal Chemistry-Anti-Cancer Agents). 2016 Dec 1;16(12):1512-22.
14. van Blitterswijk WJ, Verheij M. Anticancer alkylphospholipids: mechanisms of action, cellular sensitivity and resistance, and clinical prospects. Current pharmaceutical design. 2008 Jul 1;14(21):2061-74.
15. Jiménez-López JM, Ríos-Marco P, Marco C, Segovia JL, Carrasco MP. Alterations in the homeostasis of phospholipids and cholesterol by antitumor alkylphospholipids. Lipids in health and disease. 2010 Mar 25;9(1):33.
16. Kanwal K, Batool A, Nasim M. Cytotoxic effects of alkyl-phospholipids (Erufosine and Perifosine) in combination with cell cycle check point inhibitor (ATM) in breast cancer cells. Biomedical Current Insights. 2024 Dec 28;1(1):13-22.
17. Gududuru V, Hurh E, Durgam GG, Hong SS, Sardar VM, Xu H, Dalton JT, Miller DD. Synthesis and biological evaluation of novel cytotoxic phospholipids for prostate cancer. Bioorganic & medicinal chemistry letters. 2004 Oct 4;14(19):4919-23.
18. Nieto-Miguel T, Gajate C, Mollinedo F. Differential targets and subcellular localization of antitumor alkyl-lysophospholipid in leukemic versus solid tumor cells. Journal of Biological Chemistry. 2006 May 26;281(21):14833-40.
19. Torrens-Mas M, Collado-Solé A, Sola-Leyva A, Carrasco-Jiménez MP, Oliver J, Pons DG, Roca P, Sastre-Serra J. Mitochondrial functionality is regulated by alkylphospholipids in human colon cancer cells. Biology. 2023 Nov 22;12(12):1457.
20. Vink SR, van Blitterswijk WJ, Schellens JH, Verheij M. Rationale and clinical application of alkylphospholipid analogues in combination with radiotherapy. Cancer treatment reviews. 2007 Apr 1;33(2):191-202.
21. van der Luit AH, Vink SR, Klarenbeek JB, Perrissoud D, Solary E, Verheij M, van Blitterswijk WJ. A new class of anticancer alkylphospholipids uses lipid rafts as membrane gateways to induce apoptosis in lymphoma cells. Molecular cancer therapeutics. 2007 Aug 1;6(8):2337-45.
22. Richardson PG, Eng C, Kolesar J, Hideshima T, Anderson KC. Perifosine, an oral, anti-cancer agent and inhibitor of the Akt pathway: mechanistic actions, pharmacodynamics, pharmacokinetics, and clinical activity. Expert opinion on drug metabolism & toxicology. 2012 May 1;8(5):623-33.
23. Carnero A, Blanco-Aparicio C, Renner O, Link W, Leal JF. The PTEN/PI3K/AKT signalling pathway in

cancer, therapeutic implications. Current cancer drug targets. 2008 May 1;8(3):187-98.
24. Gills JJ, Dennis PA. Perifosine: update on a novel Akt inhibitor. Current oncology reports. 2009 Mar;11(2):102-10.
25. Fensterle J, Aicher B, Seipelt I, Teifel M, Engel J. Current view on the mechanism of action of perifosine in cancer. Anti-Cancer Agents in Medicinal Chemistry-Anti-Cancer Agents). 2014 May 1;14(4):629-35.
26. Hideshima T, Catley L, Yasui H, Ishitsuka K, Raje N, Mitsiades C, Podar K, Munshi NC, Chauhan D, Richardson PG, Anderson KC. Perifosine, an oral bioactive novel alkylphospholipid, inhibits Akt and induces in vitro and in vivo cytotoxicity in human multiple myeloma cells. Blood. 2006 May 15;107(10):4053-62.
27. Papa V, Tazzari PL, Chiarini F, Cappellini A, Ricci F, Billi AM, Evangelisti C, Ottaviani E, Martinelli G, Testoni N, McCubrey JA. Proapoptotic activity and chemosensitizing effect of the novel Akt inhibitor perifosine in acute myelogenous leukemia cells. Leukemia. 2008 Jan;22(1):147-60.
28. Unger C, Berdel W, Hanauske AR, Sindermann H, Engel J, Mross K. First-time-in-man and pharmacokinetic study of weekly oral perifosine in patients with solid tumours. European journal of cancer. 2010 Mar 1;46(5):920-5.
29. Floryk D, Thompson TC. Perifosine induces differentiation and cell death in prostate cancer cells. Cancer letters. 2008 Aug 8;266(2):216-26.
30. Fei HR, Chen G, Wang JM, Wang FZ. Perifosine induces cell cycle arrest and apoptosis in human hepatocellular carcinoma cell lines by blockade of Akt phosphorylation. Cytotechnology. 2010 Oct;62(5):449-60.
31. Deng S, Leong HC, Datta A, Gopal V, Kumar AP, Yap CT. PI3K/AKT signaling tips the balance of cytoskeletal forces for cancer progression. Cancers. 2022 Mar 24;14(7):1652.
32. Al Sawah E, Chen X, Marchion DC, Xiong Y, Ramirez IJ, Abbasi F, Zgheib NB, Chon HS, Wenham RM, Apte SM, Judson PL. Perifosine, an AKT inhibitor, modulates ovarian cancer cell line sensitivity to cisplatin-induced growth arrest. Gynecologic Oncology. 2013 Oct 1;131(1):207-12.
33. Zhang C, Li M, Zhu M. Phosphatidylinositol-3-kinase/Protein Kinase B Signaling Pathway: A Pivotal Factor for Stimulating Multidrug Resistance in Hepatocellular Carcinoma Cells. Gastroenterology & Hepatology Letters. 2021 Mar 26;3(1):1-1.
34. Kumar A, Fillmore HL, Kadian R, Broaddus WC, Tye GW, Van Meter TE. The alkylphospholipid perifosine induces apoptosis and p21-mediated cell cycle arrest in medulloblastoma. Molecular Cancer Research. 2009 Nov 17;7(11):1813-21.
35. Patel V, Lahusen T, Sy T, Sausville EA, Gutkind JS, Senderowicz AM. Perifosine, a novel alkylphospholipid, induces p21WAF1 expression in squamous carcinoma cells through a p53-independent pathway, leading to loss in cyclin-dependent kinase activity and cell cycle arrest. Cancer research. 2002 Mar 1;62(5):1401-9.
36. Masood M, Numan A, Mahmood S. Effects of synthetic alkyl-phospholipid (Perifosine) on survival and cell cycle relevant genes of hepatocellular carcinoma cells. Biomedical Current Insights. 2024 Dec 27;1(1):23-8.
37. Li Y, Guo Y, Tang J, Jiang J, Chen Z. New insights into the roles of CHOP-induced apoptosis in ER stress. Acta Biochim Biophys Sin. 2014 Aug 1;46(8):629-40.

Use of generative AI: Artificial intelligence (AI), including ChatGPT (OpenAI), was used during the preparation of this manuscript to assist with language editing, organization, and drafting of selected sections. The authors critically reviewed, verified, and revised all AI-assisted content and took full responsibility for accuracy, originality, interpretation, and scientific integrity of the final manuscript. AI tools were not used to generate or fabricate experimental data, results, or scientific findings.

Author Contributions: MN performed experiments and wrote the draft, IA analyzed the draft and prepared the figures, IN helped with literature and draft writing.

Competing Interests: Authors declare no competing interests.

Ethical Statement: Not Applicable

Financial Support: No specific grant was availed for this research.

Data Availability: The datasets generated and/or analyzed during the current study are available from the corresponding author on reasonable request.